

SHORT-PERIOD INTENSITY OSCILLATIONS IN THE SOLAR CORONA OBSERVED DURING THE TOTAL SOLAR ECLIPSE OF 26 FEBRUARY 1998

RAMANATH COWSIK, JAGDEV SINGH, A. K. SAXENA, R. SRINIVASAN and
A. V. RAVEENDRAN

Indian Institute of Astrophysics, Bangalore, 560034, India

(Received 23 March 1999; accepted 29 April 1999)

Abstract. Encouraged by the detection of high-frequency, low-amplitude continuum intensity oscillations in the solar corona during the total solar eclipse of 1995, we designed and fabricated a six-channel photometer incorporating low-noise Hamamatsu R647 photomultipliers. Fast photometry at five different locations in the solar corona was performed at Don Bosco Mission, Venezuela during the total solar eclipse of 26 February 1998. Three interference filters with passbands of about 150 Å and centered around 4700, 4900, and 5000 Å were used. The photometric data were recorded at a rate of 20 Hz in three channels and 50 Hz in the remaining three channels. The power spectrum analysis of one of the channels that recorded appreciable counts indicates the existence of intensity oscillations in the frequency range 0.01–0.2 Hz. A least-squares analysis yields 90.1, 25.2, and 6.9 s periods for the three prominent components which have amplitudes in the range 0.5–3.5% of the coronal brightness. These periods and their amplitudes are similar to those detected in the coronal intensity oscillations during the 1995 eclipse.

1. Introduction

A number of experiments conducted recently on-board SOHO have given new insights into the physical and dynamical characteristics of the solar corona. The existence of intensity and velocity oscillations, and the nature of these oscillations still need to be investigated because of their bearing on the mechanism of coronal heating (Porter, Klimchuk, and Sturrock, 1994; Pasachoff and Ladd, 1987; Zirker, 1995; Cargill, 1995). We have listed the earlier investigations of coronal oscillations with coronagraphs and space-borne instruments, and during total solar eclipses in a previous paper (Singh *et al.*, 1997) in which the detection of continuum intensity oscillations in the solar corona is reported. The fast photometry at a single location in the solar corona obtained by us during the total solar eclipse of 24 October 1995 indicated oscillations in the frequency range 0.02–0.2 Hz with amplitudes between 0.2 and 1.3% of the coronal brightness. We had recorded the intensities at a rate of 20 Hz with a 250 Å passband filter centred around 5500 Å. Encouraged by the result of this experiment and to confirm these oscillations we decided to fabricate a multichannel photometer incorporating low dark current, low noise photomultiplier tubes to conduct experiments during the future total solar



TABLE I
Characteristics of the multichannel photometer

Channel No.	Filter		Coronal region		Counts per second		
	Central λ (\AA)	Passband (\AA)	Position angle($^{\circ}$)	R_{\odot}	Dark mean	Dark scatter	Totality mean
1	4861	175	215	1.2	13.2	3.6	3309.9
2	4861	175	215	2.0	24.3	4.6	594.8
3	4160	160	125	1.2	12.3	4.0	9995.5
4	4700	190	35	1.2	76.9	9.4	2064.5
5	4700	190	35	2.0	106.8	10.4	669.8

eclipses. Here we report the results of fast photometry of continuum radiation performed at 5 different locations in the corona during the total solar eclipse of 26 February 1998.

2. Instrumentation

A stepper motor-driven coelostat mirror of 30 cm aperture and another mirror of 20 cm aperture were used to feed the sunlight to a horizontal telescope objective of 20 cm aperture and 300 cm focal length. For the observations a multichannel photometer was specially designed and fabricated in our laboratories using six R647 photomultiplier tubes from Hamamatsu of Japan. The dead time of these photomultiplier tubes is 9 ns. Five channels of the photometer were fed by light from five different regions in the solar corona using small reflecting prisms. The 200 μm aperture diaphragms kept at the focus of the telescope objective isolated coronal regions whose positions are listed in Table I. Each aperture subtended an angle of 18 arc sec in the sky. Three interference filters, each capable of covering two diaphragms, were mounted in front of the diaphragms. The relevant details of the interference filters used are also given in Table I. The light from a small central portion of the objective was diverted through a set of prisms and lenses to make a tiny image of the solar corona up to 1.8 solar radii, and to image on the sixth photomultiplier tube. Each channel had a Fabry lens in front of the photomultiplier tube to reduce the problems associated with the non-uniform sensitivity across the surface of the photocathode. The photomultiplier tubes were mounted in magnetically and electrically shielded boxes to avoid the interference from nearby electronic circuits with the signal. The pre-amplifier-discriminators with a bandwidth of 600 MHz were supplied by Romualdas Kalytis, Astronomical Observatory of Vilnius University. The data acquisition was made using the software ‘Quilt-9’ developed by Prof. Edward Nather of University of Texas at Austin,

USA for the time series photometric study of the pulsating variables. The software permits each of the two laptop computers used to collect data from three channels at a maximum rate of 60 Hz. The photons were detected with the cathodes of the photomultiplier tubes kept at ground potential.

3. Observations

A team from Indian Institute of Astrophysics, Bangalore, India went to Venezuela and set up the experiment in the playground of Don Bosco Mission, Carrasquero (latitude $11^{\circ}03'62''$ N, longitude $72^{\circ}03'23''$ W) near Maracaibo. The longitude axis of the coelostat mirror was a little misaligned and the tracking speed adjusted so that there was no noticeable drift of the solar image for about 15 min around the time of totality. It had been planned to select two regions on the eastern part of the solar corona at 1.2 and 2.0 solar radii, two on the western part of the corona at similar distances and one on the southern part at 1.2 solar radii. The east–west direction was chosen to get strong signals due to the possible presence of some streamers or active structures and to detect any drift or oscillations, if present, in the image during the observations. The solar image had been monitored visually on many days at the Institute campus before the eclipse expedition and at the eclipse site, and no oscillations had been detected in the image during the observations. At the eclipse site the photomultiplier tubes could not be positioned at the positions planned earlier. The coordinates of the regions in the corona observed in the different channels are given in Table I. The final centring of the image with respect to the photomultiplier tubes was done about 10 min before the total eclipse. There was no drift of the solar image during the observations.

The Hamamatsu R647 photomultiplier tubes, which stabilize within 10 min, do not need cooling below the ambient temperature since they have low dark currents. The HT supply to the tubes was put on about 3 hr before the beginning of the solar eclipse. In order to check the performance of the instrumental setup, including the behaviour of electronic components, several test runs on the dark counts were made before and after the total phase of eclipse. A number of tests with the sky brightness were also performed during evening twilight on three days prior to the event. There was a small difference in the average dark counts recorded in the morning and noon times due to a difference in the ambient temperatures; however, the spreads in the dark counts did not show any noticeable change.

The dark counts before and after the total eclipse were found to be between 50 and 120 per second for different tubes with the scatter in the range of 15–35 per second. Though the data acquisition program was initiated right at the beginning of the totality phase, the photometer shutter was opened 5 s later to avoid the intense light entering the sixth channel and damaging the photomultiplier tube. The shutter was closed 5 s before the expected end of totality for the same reasons. The coronal intensity data were obtained for about 190 s. The photon counts were recorded

continuously with an integration time of 20 ms for the first three channels and 50 ms for the other three channels. It may be noted that the sky was covered with low clouds till noon time, two hours before the totality. Fortunately, the clouds began to disappear as a slow wind started blowing and the sky became completely clear about an hour before the totality. There were no clouds visible during the totality phase and the transparency appeared good all over the sky till evening.

4. Data Analysis and Results

In Table I we also list the average counts per second for the five channels looking at five different locations in the solar corona. The counts varied in different channels because of the positionings of the diaphragms with respect to the coronal structures and the exponential fall in the coronal intensity with distance from the centre of the Sun. The registered counts are considerably less than the expected values based on the observations of the Moon with the same instrumental setup. We could not resolve this discrepancy. We have determined the locations of our observed regions with respect to the coronal structures from the high spatial resolution broadband pictures of solar corona taken by V. Rušin at the same camp. The channels 2 and 5 covered regions at 2 solar radii and were away from coronal streamers. These channels show rather low counts, and due to the intrinsic scatter in the dark counts permit us to study only the intensity variations greater than 5% of the coronal brightness. We do not see any variations in the intensity in these channels at this level. The channel 4, which covered a region in the north-east quadrant at 1.2 solar radii, happened to lie just outside a coronal streamer, and the channel 1 unfortunately covered a region in the cavity of a large streamer structure in the south-west quadrant. These channels gave reasonable counts during the total eclipse phase but do not show any immediately noticeable variations with periods greater than 10 s. To detect the short-period variations with low amplitudes we have performed a Fourier analysis of these two data sets using the technique of Discrete Fourier Transform (DFT). Both of the resulting amplitude spectra of coronal brightness are found to be noisy; but they do indicate an excess power around a frequency of 0.5 Hz at a marginal level of 2σ .

The channel 3, which monitored a region in the corona at 1.2 solar radii, recorded about 200 counts in 20 ms on an average. Figure 1, which is a plot of the data in this channel, clearly shows the modulations in the intensity. This channel happened to look at a portion of a moderately intense coronal structure. In the following we analyze and discuss the data recorded in this channel in more detail. Figure 1 indicates that the observed counts during the totality varied with an amplitude of about 400 counts per second, and with a mean value of about 10 000 counts per second, this corresponds to a modulation of coronal intensity at 4% level. The figure also indicates a gradual increase in intensity at 1% level from the beginning to the end of totality. The increase may be due to either variations in the coronal intensity

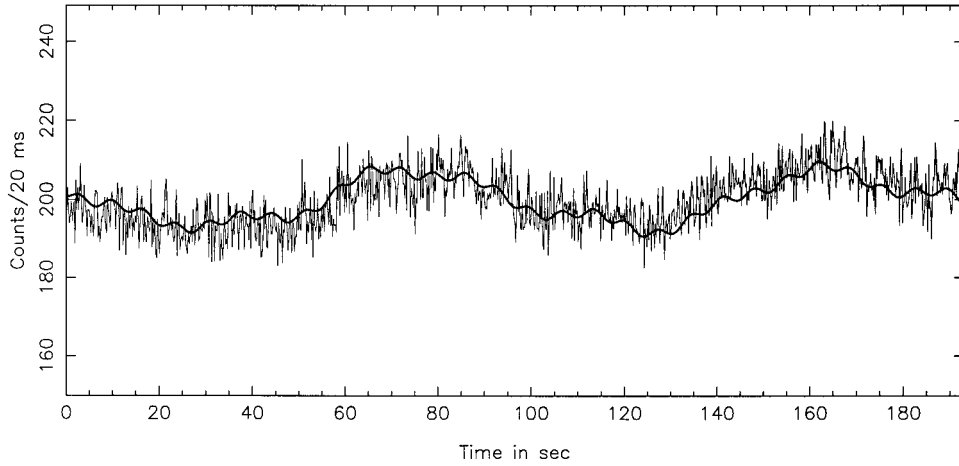


Figure 1. The spiky curve shows the raw data with a temporal resolution of 200 ms and the smooth curve that is computed using the 3 frequency components listed in Table II. The time plotted along x -axis is reckoned from 18:03:50 UT.

TABLE II

Periodicities identified in the data (mean of input data = 199.9 ± 0.01 counts/20 ms)

No.	Frequency (Hz)	Period (s)	Amplitude % coronal brightness	Time of maximum (s)
1	0.0111 ± 0.0001	90.1 ± 0.8	3.51 ± 0.08	75.5 ± 0.5
2	0.0397 ± 0.0003	25.2 ± 0.2	0.83 ± 0.08	3.3 ± 0.4
3	0.1446 ± 0.0004	6.9 ± 0.1	0.54 ± 0.08	2.8 ± 0.2

with time-scales significantly longer than the data length, or a slow increase in the sky transparency. In addition to the above mentioned modulation at 4% intensity level one can see short period intensity variations with very low amplitudes. In order to detect and isolate the periodic components, the string of 9610 data points was Fourier analyzed using the DFT method. The amplitude spectrum of coronal brightness shown in Figure 2 indicates the presence of four peaks which have amplitudes above 3σ level. The first peak at the low frequency end with a period significantly longer than 190 s is due to the long-term trend in the data. The second peak around 0.01 and having the largest amplitude is because of the long period variation clearly seen in intensity data. There are two other peaks around 0.04 and 0.15 Hz which have significant amplitudes above the noise level. We have used the method of least-squares to derive the frequencies, amplitudes and the time of

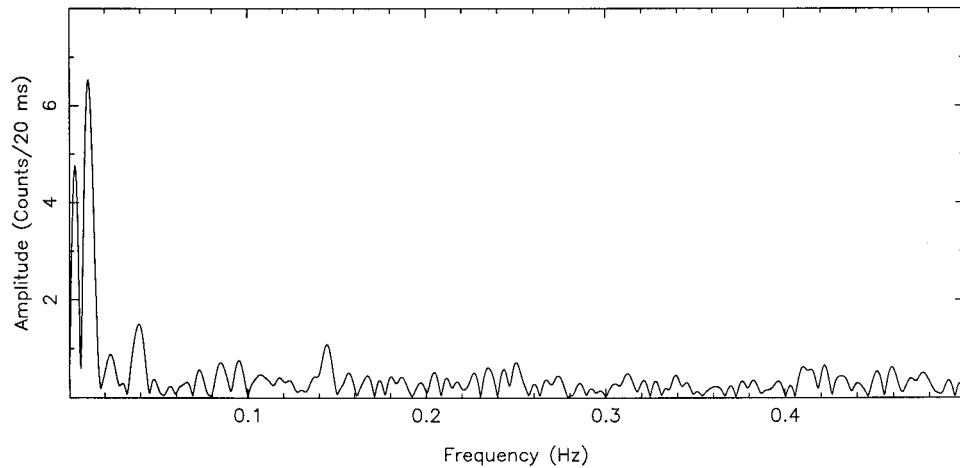


Figure 2. Amplitude spectrum in the frequency interval 0–0.5 Hz computed from the raw data plotted in Figure 1.

maximum of these three significant components identified in the power spectrum. These constitute 9 unknowns which were solved simultaneously using the original data and the values thus obtained are given in Table II along with their probable errors; the mean brightness level was also treated as an unknown in the least square solution. The coronal brightness computed using the frequency components listed in Table II and the value of mean intensity is also plotted in Figure 1. The agreement between the computed and observed brightness variations is reasonably good over the entire data length. Assuming the variations as sinusoidal in nature we have computed the residuals from the data after the removal of the contributions due to the above mentioned three components. The amplitude spectrum of the residuals shown in Figure 3 indicates the absence of peaks at the frequencies listed in Table II and appears noisy except for the peak corresponding to the long-term trend in the data. The amplitude spectrum plotted in Figure 2, derived from the original data set, is noisy, and one may be skeptical about the existence of the periods in the intensity modulation mentioned above. Therefore, we show in Figure 4 the intensity data with a temporal resolution of one second and in Figure 5 the power spectrum of this data which clearly indicates the existence of intensity variations with periods 90.1, 25.2, and 6.9 s. Further, the amplitude spectrum computed after randomizing the raw data is found to be noisy and does not show excess power at any particular frequency.

5. Discussion

In the previous paper (Singh *et al.*, 1997) we have discussed in detail the effects of various factors, such as the variations in the tracking rate of the coelostat, modu-

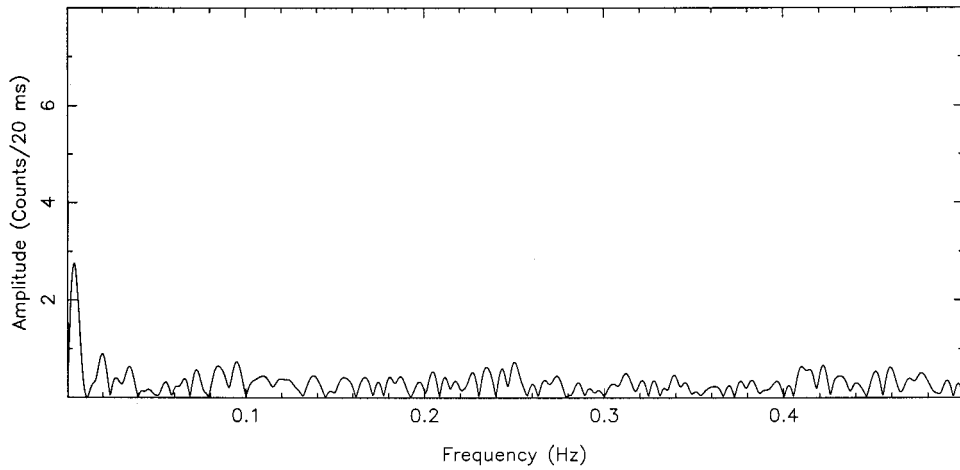


Figure 3. Amplitude spectrum in the frequency range 0–0.5 Hz computed from the residuals obtained after the removal of the contributions due to the 3 components given in Table II from the data. Note the absence of peaks corresponding to the 3 components.

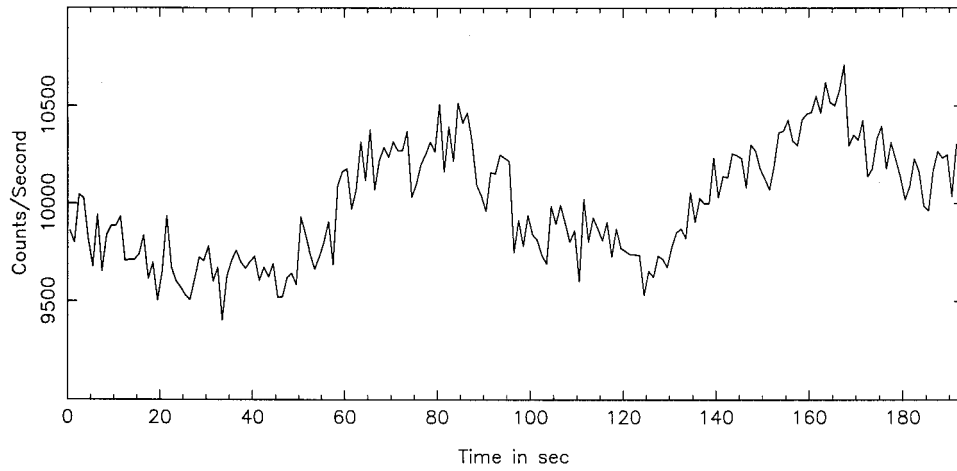


Figure 4. Observed intensity variations with a temporal resolution of 1 s.

lation by the associated electronics, variation in sky transparency, and atmospheric seeing in the observed power spectrum. To rule out the possibility that the frequency components identified in the power spectrum could be due to any one of the above factors, we have also performed the power spectrum analyses of the dark counts recorded on several occasions and the sky brightness observed during the morning and evening times on a few days. The absence of any significant periodicity in the power spectra indicate that the instrumental setup did not introduce any periodic modulations in the signal. The power spectrum of the sum of counts in the remaining four channels, namely 1, 2, 4, and 5 does not show excess power at

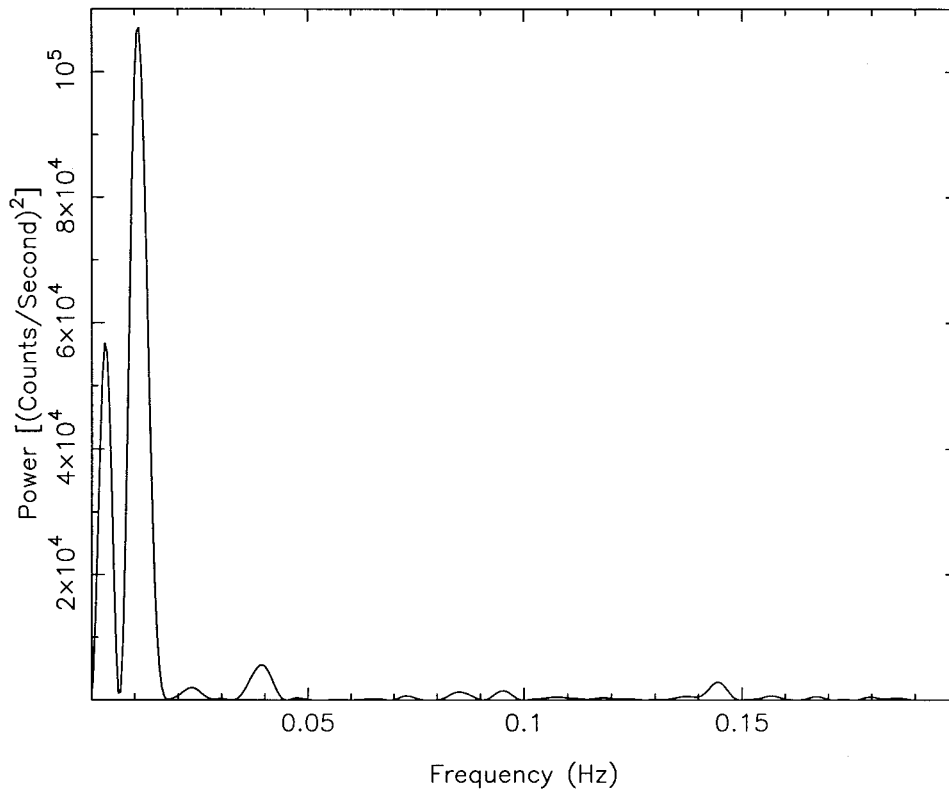


Figure 5. Power spectrum of the data plotted in Figure 4 appears less noisy and clearly shows the 3 peaks corresponding to the components listed in Table II above 3σ level.

any frequency, implying that the periodic modulation observed in channel 3 does not arise from a modulation in the atmospheric transparency during totality. The brightness variation due to the effect of seeing, which could be around 2 arc sec, is expected to be very small and random across the 18 arc sec covered by the $200\ \mu\text{m}$ diaphragm. Further, the intensity variations due to the seeing effects usually lie in the frequency interval 5–10 Hz, and all the three components quoted above have frequencies < 0.15 Hz. None of the periods given in Table II is associated with the anti-backlash gear system used in the coelostat drive (Singh *et al.*, 1997). Observations were also obtained by positioning an aperture slightly away from the solar limb so as to provide an inhomogeneous sky background which rapidly varied with increasing distance from the solar limb. Under such a condition any oscillations in the coelostat are expected to cause modulations in the observed intensity. However, the corresponding power spectrum does not show any significant periodicity.

Singh *et al.* (1997) reported intensity variations in continuum at six frequencies in the interval 0.02–0.2 Hz with amplitudes between 0.20 and 1.31% of the coronal brightness from the observations made during the total solar eclipse of 24 October

TABLE III

Computed fluxes for slow and fast modes in active region coronal structures for $B = 30$ G

Period (s)	Slow mode F (erg cm ⁻² s ⁻¹)	Fast mode F (erg cm ⁻² s ⁻¹)
90.1	20.6×10^4	11.7×10^7
25.2	4.8×10^4	2.8×10^7
6.9	3.1×10^4	1.8×10^7

1995. The total intensity variation was of the order of 6% of coronal brightness. They could do a thorough analysis of the data because of the large signal-to-noise ratio they achieved. From an analysis of the soft X-ray images taken with SXT on *Yokoh*, McKenzie and Mullan (1997) have also found the existence of waves with periods in the range 5–60 s in the solar corona. The present data indicate similar variations in the continuum coronal intensity. The intensity variation with a period of 90.1 s and an amplitude of 3.5% of coronal brightness may be compared with the values of 56.5 s and 1.3% observed during the 1995 eclipse. The other two frequency components have periods and amplitudes similar to those observed during the 1995 eclipse. The periods and amplitudes of intensity oscillations may depend on the size, shape, temperature, density or magnetic field of the observed coronal structure.

Coronal structures may undergo three types of oscillations – non-compressional Alfvén waves, and the compressional slow and fast magnetosonic waves (Singh *et al.*, 1997). Alfvénic oscillations are essentially velocity oscillations and do not cause any density fluctuations. The compressional modes may reveal themselves in the form of intensity oscillations through a variation of emission measure. Our data show intensity oscillations which could be interpreted either as slow mode, or fast mode. Theoretical studies of coronal oscillations (Porter, Klimchuk, and Sturrock, 1994; Zirker, 1995) indicate a wide range of periods for these oscillations.

We have observed intensity oscillations with periods and amplitudes as given in Table II in a region of a coronal streamer. Therefore, to identify these waves we choose the canonical parameters for active region of the Sun from Porter, Klimchuk, and Sturrock (1994). For the active region at 1.2 solar radii, we take the electron density $n_e = 5 \times 10^9$ cm⁻³, the magnetic field $B = 30$ G, and the electron temperature $T_e = 2.5 \times 10^6$ K. More details on the various parameters can be seen in Singh *et al.* (1997). The computed fluxes F for slow and fast modes for the observed periods and amplitudes of coronal intensity oscillations are listed in Table III. It follows from the table that fast mode oscillations in active regions can provide enough flux for the heating of solar corona, as also concluded by Porter,

Klimchuk, and Sturrock (1994). These findings agree with those of Singh *et al.* (1997) from the observations made during the 1995 eclipse.

In summary, we may say that we have confirmed the existence of short-period oscillations in the frequency range 0.01–0.2 Hz in the coronal brightness. The intensity oscillations appear to be prominent in closed field coronal structures or coronal streamers; this needs to be confirmed from further observations.

Acknowledgements

We thank the staff of Photonics, Mechanical and Electronic Laboratories, Stores and Administration, who helped us at various stages of this expedition. We also thank our colleagues who took keen interest in this experiment. We thank Prof. Jeanette Stock and her students for taking care of all our needs at the campsite. Mr B. N. Ashoka helped us in the initial installation and testing of the photometric system. Finally we thank Prof. V. Rušin for sending us the picture of solar corona before its publication and Prof. Edward Nather of University of Texas at Austin, USA for permitting us to use the data acquisition software ‘Quilt-9’.

References

- Cargill, P. J.: 1995, in J. R. Kuhn and M. J. Penn (eds.), *Infrared Tools for Solar Astrophysics: What Is Next?*, World Scientific Publishing Co. Ltd., Singapore, p. 17.
- McKenzie, D. E. and Mullan, D. J.: 1997, *Solar Phys.* **176**, 127.
- Pasachoff, J. M. and Ladd, E. F.: 1987, *Solar Phys.* **109**, 365.
- Porter, L. J., Klimchuk, J. A., and Sturrock, P. A.: 1994, *Astrophys. J.* **435**, 482.
- Singh, J., Cowsik, R., Raveendran, A. V., Bagare, S. P., Saxena, A. K., Sundararaman, K., Krishan, V., Naidu, N., Samson, J. P. A., and Gabriel, F.: 1997, *Solar Phys.* **170**, 235.
- Zirker, J. B.: 1995, in J. R. Kuhn and M. J. Penn (eds.), *Infrared Tools for Solar Astrophysics: What Is Next?*, World Scientific Publishing Co. Ltd., Singapore, p. 13.